

RADIATIVELY COUPLED WAVEGUIDE CONCEPT FOR AN INTEGRATED MAGNETO-OPTIC CIRCULATOR

M. Lohmeyer, M. Shamonin, N. Bahlmann, P. Hertel, H. Dötsch
Department of Physics, University of Osnabrück, 49069 Osnabrück, Germany

ABSTRACT

Three-guide couplers with multimode central waveguides allow for remote coupling between optical channels. A simple three mode approximation turns out to be sufficient for the description of the main features of the power transfer behavior. The specific form of the relevant modes suggests the design of integrated optical isolators and circulators based on magnetic garnet materials. These novel devices are superior to conventional nonreciprocal couplers with respect to the total length and admissible fabrication tolerances. We characterize the isolation performance and the transmission loss for the proposed devices by propagating mode simulations and estimate the influence of geometry parameter deviations.

INTRODUCTION

The majority of integrated optical isolator proposals comprises two waveguide ports, which are connected for light propagation in the direction of transmission. In the opposite direction the power is either damped by a polarizer or radiated into the surrounding. In contrast the concept of the nonreciprocal coupler [1, 2] is suitable for the realization of circulator devices, since the blocked power remains well confined in its own output waveguide. For current magneto-optic materials with undesirably high optical losses, the conventional X-coupler has the drawback of large total length and prohibitively strict fabrication tolerances. In this paper we show how this can be overcome by insertion of a third multimode rib, for both planar and rib waveguide devices.

RADIATIVELY COUPLED WAVEGUIDES

Fig. 1 depicts the three waveguide couplers discussed in this paper. For numerical modeling we regard the entire structure between $z = 0$ and $z = L$ as a single lossless multimode waveguide. Interference of its supermodes determines the power transfer between the outer waveguides.

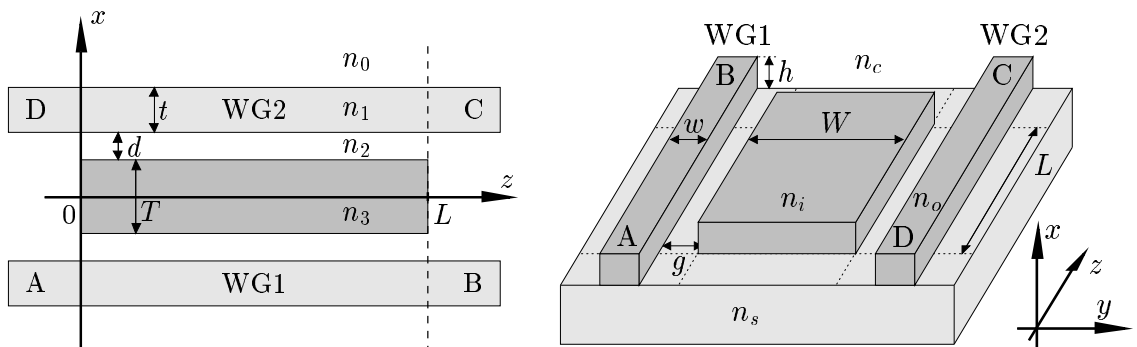


Figure 1: Geometries of the planar (left) and rib waveguide devices (right). The central layer or the central rib, resp., couples two identical outer waveguides WG1 and WG2. The structures are to be considered four port devices with input and output channels A to D.

We start with a look at the dispersion characteristics, focusing on planar devices first. For given vacuum wavelength $\lambda = 2\pi/k$ and polarization state, each outer waveguide supports one mode with a propagation constant denoted β_* . To achieve remote coupling, the isolated central waveguide must support modes with propagation constants beyond this level. Then the effective

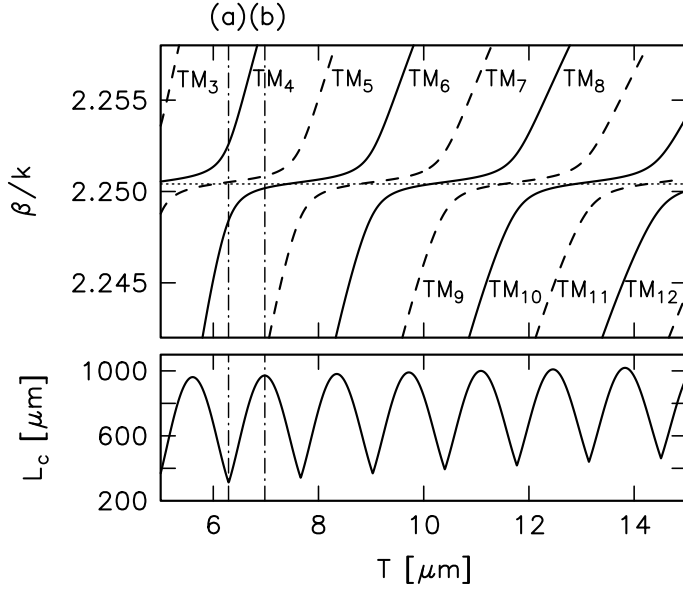


Figure 2: Effective indices β/k (top) and the corresponding coupling length L_c (bottom) for TM-polarized modes versus the thickness T of the central layer in a planar structure. The dotted line indicates the level $\beta_*/k = 2.25041$ of the single outer waveguide's TM mode. Only a small fraction of the region allowed for modal indices is displayed. Parameters are: $\lambda = 1.3 \mu\text{m}$, $t = 0.8 \mu\text{m}$, $d = 0.8 \mu\text{m}$, $n_0 = n_2 = 2.18$, $n_1 = n_3 = 2.30$.

mode indices of the entire structure typically exhibit a dependence on the coupling layer thickness T as depicted in Fig. 2.

For each thickness T there are either two or three propagation constants close to β_* . The corresponding modes show large field amplitudes in the outer guiding regions (see Fig. 3), thus carrying most of the power if the structure is excited by the mode of one outer waveguide. For the parameters given for Fig. 2 and T up to $15 \mu\text{m}$ this amount is larger than 90% for the three modes with propagation constants next to β_* . Therefore we focus at first on the interference between only these three most excited modes.

The two of them with the smaller difference between their propagation constants β_s, β_a , define a characteristic length $L_c = \pi/|\beta_s - \beta_a|$. L_c can be regarded a coupling length if either the power carried by the third mode is negligible, or if the propagation constant of the third mode fits properly to enable complete power transfer. We have found that points T with the relevant propagation constants properly spaced occur frequently to justify calling L_c the coupling length for all T . This is further elaborated in [3].

Due to the harmonic dependence of the modes on the transverse coordinate x in the coupling region, L_c shows a nearly periodic dependence on T as well. Around the minima of $L_c(T)$, three modes determine the coupling behaviour, next to the maxima only two modes have to be considered. We call these regions the three- and two-mode regime, respectively. Two examples have been marked in Fig. 2, Fig. 3 shows the relevant mode field profiles.

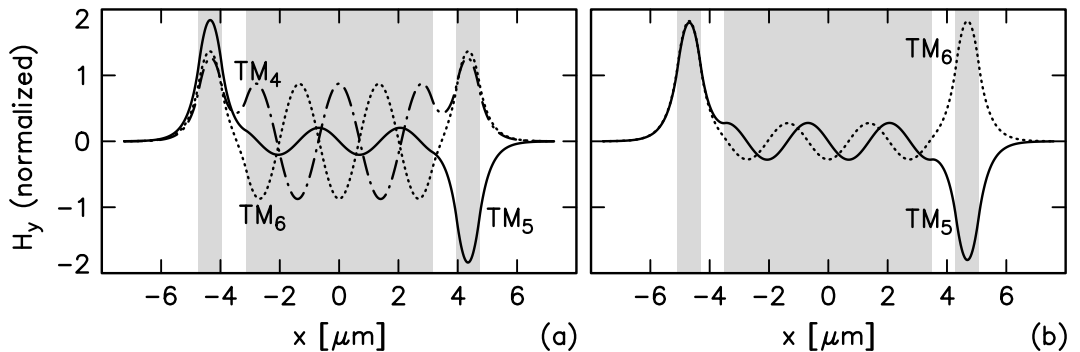


Figure 3: Mode field profiles for coupling layer thicknesses $T = 6.29 \mu\text{m}$ (a) and $T = 6.98 \mu\text{m}$ (b), corresponding to the three- (a) and two-mode regime (b) marked in Fig. 2.

In a realistic simulation all normalized modes ψ_j of the entire structure have to be considered. Denote by β_j the corresponding propagation constants and by ϕ_1, ϕ_2 the normalized modes of

WG1 and WG2. Suppose ϕ_1 is launched into the coupling region at $z = 0$. Neglecting reflections at input and output, the relative power transmitted to waveguide k at $z = L$ is given by $P_k(L) = |\sum_j \langle \phi_k, \psi_j \rangle \langle \psi_j, \phi_1 \rangle \exp(-i\beta_j L)|^2$. $\langle \cdot, \cdot \rangle$ denotes the appropriate scalar product. It is a very good approximation to restrict the sum to guided modes. At least for the planar structures in this paper we have found $P_1(0) \geq 0.999$, thus these devices show only low radiation losses at input and output. Reflections should be of the same order of magnitude, i.e. negligible. Note that waveguide bends as needed for the conventional coupler can be completely avoided.

MAGNETO-OPTIC LAYERS

We will now assume that some layers have a linear magneto-optic effect with the static magnetization adjusted in the y direction (see Fig. 1). In these regions the permittivity tensor $\hat{\epsilon}$ reads

$$\hat{\epsilon} = \begin{pmatrix} n^2 & 0 & -i\xi \\ 0 & n^2 & 0 \\ i\xi & 0 & n^2 \end{pmatrix}, \quad (1)$$

where the small off-diagonal elements are related to the specific Faraday rotation Θ_F and refractive index n by $\xi = n\lambda\Theta_F/\pi$. ξ enters via a perturbational expression [4]. While TE-like modes are not affected in first order, the propagation constants of TM modes are shifted by an amount $\delta\beta$. For a two-dimensional piecewise constant profile with discontinuity lines in $x = x_j$, $y_{j,0} < y < y_{j,1}$ separating permittivities $n_{j,-}$, $\xi_{j,-}$ below and $n_{j,+}$, $\xi_{j,+}$ above, the nonreciprocal phase shift can be written

$$\delta\beta = \frac{1}{2} \sum_j \int_{y_{j,0}}^{y_{j,1}} \left(\frac{\xi_{j,+}}{n_{j,+}^2} - \frac{\xi_{j,-}}{n_{j,-}^2} \right) |H_y(x_j, y)|^2 dy, \quad (2)$$

where $H_y(x, y)$ denotes the transverse magnetic field component of the TM mode in the corresponding isotropic waveguide, normalized to $\iint n^{-2} |H_y|^2 dx dy = 1$. We refer to the semivectorial approximation, neglecting the normal component H_x . In the case of planar waveguides, the second argument y and the corresponding integration must be removed.

Reversing the direction of propagation while the static magnetization remains changes the sign of ξ , thus the propagation constants for forward and backward direction differ by $2\delta\beta$. Usually the coupling lengths L_c^f and L_c^b for forward and backward propagation are different as well. An isolator results if the device length can be adjusted such that $L = lL_c^f = (l \pm 1)L_c^b$ holds for an integer number l .

Indicating by subscripts s and a the most relevant supermodes of our coupler structures, the smallest possible isolator length can be shown to be

$$L_{is} = \frac{\pi}{2|\delta\beta_s - \delta\beta_a|}. \quad (3)$$

To realize a short device, not only a large phase shift is required, but also the *difference* between the nonreciprocal phase shifts of the two modes must be as large as possible.

Note that this is the weak point of the conventional coupler: its two squared supermodes appear very similar, thus the difference in the nonreciprocal phase shifts remains small.

PLANAR DEVICES

As an example, Fig. 4 shows the squared amplitudes of the relevant supermodes in the three mode regime. The largest differences occur in the center of the outer waveguides and periodically in the central waveguide. Obviously the shortest isolating device results if the guiding regions can be manufactured from layers with opposite Faraday rotation, such that the ξ profile changes exactly at these points. This is illustrated in the bottom inset of Fig. 4.

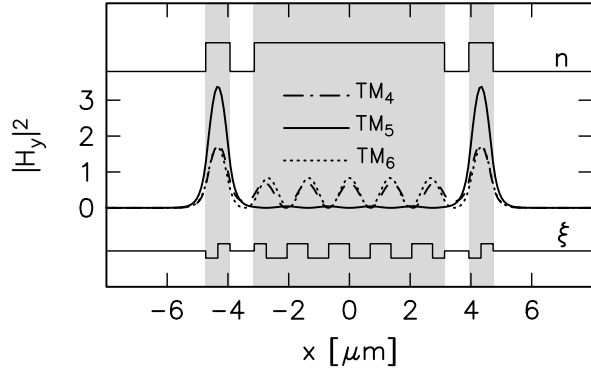


Figure 4: Field intensity for the modes of Fig. 3(a). The insets outline the corresponding refractive index profile (top) and an optimum choice for the profile of the Faraday rotation (bottom).

For such multilayer configurations, Eq. 3 evaluates to the curves of Fig. 5. Clearly, the shortest devices can be expected in the regions of the three mode regime, for periodically occurring values T . Note that Fig. 5 gives a rough estimate of the realistic device length only, since merely two modes enter Eq. 3. However, the exact numerical calculations show that close to the values indicated by Eq. 3 sets of parameters for well performing devices can be found [3].

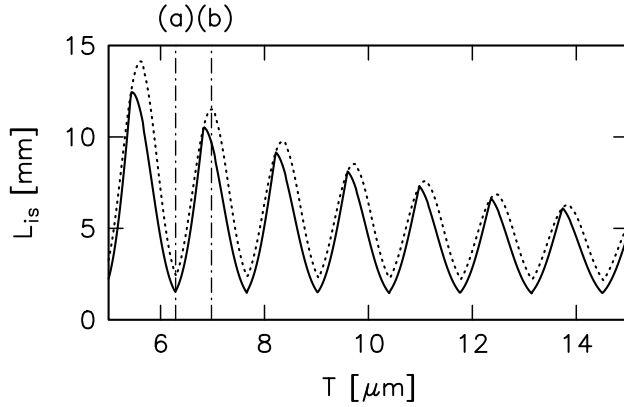


Figure 5: Isolator device length L_{is} versus the thickness T of the coupling layer. For the dotted curve, only the central layer has been modeled as a magnetic grating with alternating Faraday rotation, while for the continuous curve the outer waveguides are assumed to be double layer waveguides with opposite Faraday rotation as well. Parameters are as given for Fig. 2, $\xi = \pm 0.005$.

Fig. 6 illustrates the light propagation in one of these devices. With outer waveguides formed as double layers, each of thickness $t/2$, with opposite sign of Θ_F , and the coupling region made up of 10 layers of alternating Faraday rotation, the device achieves an isolation $10 \log_{10} P_1^f / P_1^b$ of 38 dB and a forward transmission loss $-10 \log_{10} P_1^f$ of 0.15 dB. The tolerances given in the figure caption guarantee isolation better than 20 dB and losses below 0.5 dB, where losses due to material absorption must be added.

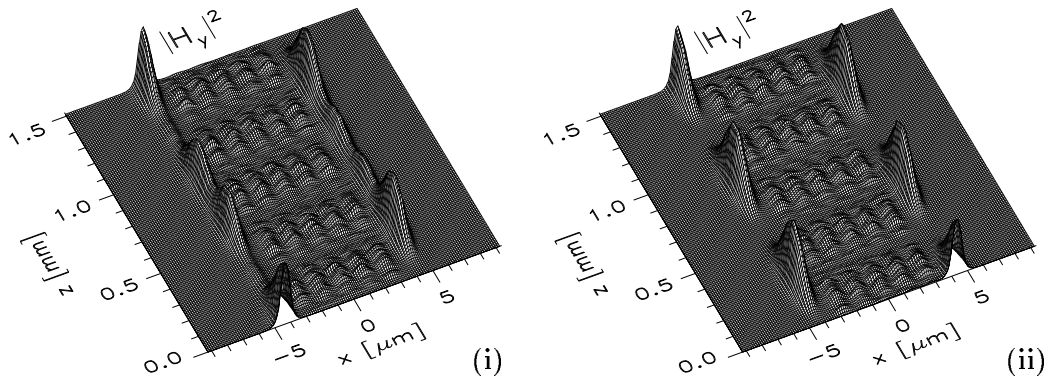


Figure 6: TM-field propagation along the planar isolator device corresponding to mark (a) in Figs. 2,3,5. (i): propagation in the direction of transmission, the mode of one outer waveguide is inserted at $z = 0$ and the power remains in the input waveguide (A to B in Fig. 1). (ii): propagation in the blocking direction, the structure is excited in $z = 1.5$ mm and the power is transferred to the opposite waveguide (transmission B to D). Parameters are as given for Fig. 2, $T = 6.261 \mu\text{m}$, $L = 1512 \mu\text{m}$, $\xi = \pm 0.005$. Tolerances: $\Delta T = \pm 5 \text{ nm}$, $\Delta L = \pm 35 \mu\text{m}$, $\Delta t = \pm 3 \text{ nm}$, $\Delta d = \pm 16 \text{ nm}$.

For comparable conventional nonreciprocal couplers ($T = 0$ in Fig. 1) the total length must be larger than 2.8 mm ($2d = 0$) or 10.5 mm ($2d = 0.8 \mu\text{m}$), with a maximum tolerance of $0.7 \mu\text{m}$ ($2d = 0$). The gap width $0.8 \mu\text{m}$ has to be maintained with a tolerance of $\pm 0.4 \text{ nm}$.

RIB WAVEGUIDE DEVICES

In somewhat more realistic 3-D structures analogous mode patterns appear. Fig. 7 illustrates the supermodes of a rib coupler in the three mode regime, generated by means of a recently proposed semivectorial mode solver [5]. The three most relevant modes corresponding to the planar profiles in Fig. 3(a) can be clearly identified.

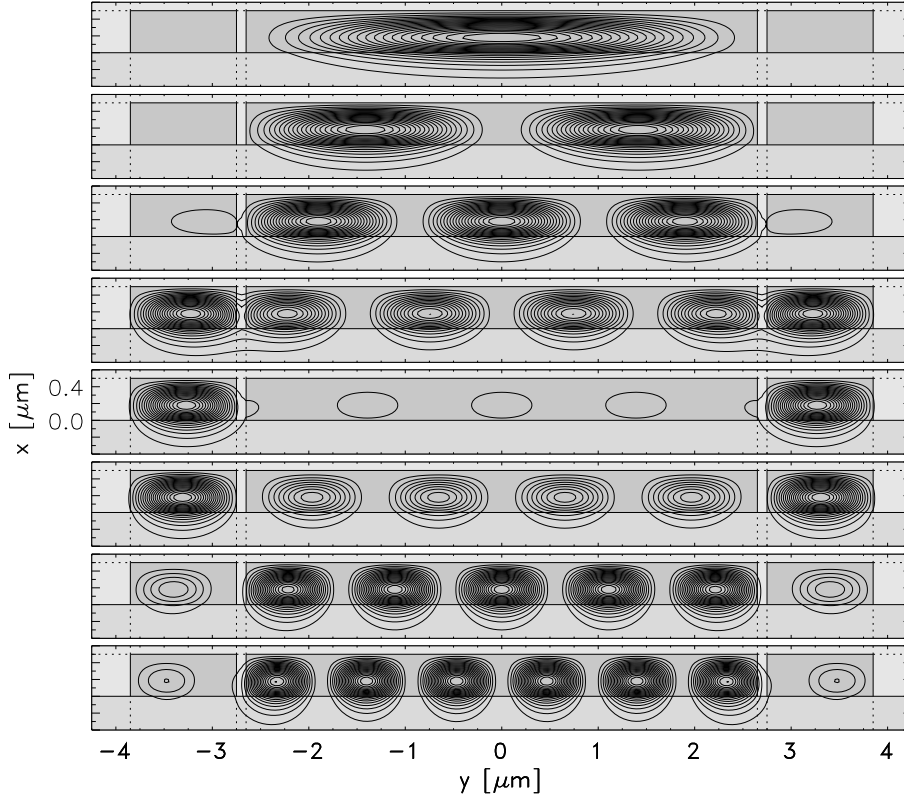


Figure 7: Mode intensity profiles for the eight TM polarized modes of a radiatively coupled waveguide structure given by the following parameters: $W = 5.3 \mu\text{m}$, $w = 1.1 \mu\text{m}$, $g = 0.1 \mu\text{m}$, $h = 0.5 \mu\text{m}$, $n_i = n_o = 2.3$, $n_s = 1.95$, $n_c = 1.0$, $\lambda = 1.3 \mu\text{m}$ (cf. Fig. 1). The contours correspond to the squared dominant magnetic field component $|H_y|^2$.

The mode shape inspires an isolator configuration as shown in Fig. 8. It does not exploit the opposite symmetry, but the strongly differing amplitudes of the relevant modes. The nonreciprocal phase shifts of the central and the surrounding mode must be as unequal as possible, therefore contrarily directed jumps in the Faraday rotation should be manufactured along the lines of the corresponding field maxima.

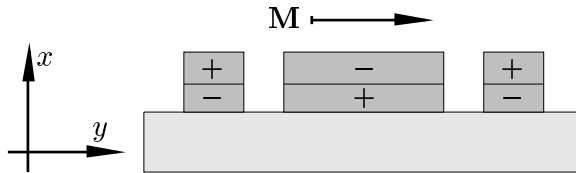


Figure 8: Concept for an TM-isolator/circulator based on radiatively coupled rib waveguides. The boundary between layers with opposite Faraday rotation (signs) should be adjusted to the maximum field amplitude.

With the central layer thickness T replaced by the width W of the central rib, the dispersion characteristic of the 3-D devices is similar to the planar case, as confirmed by Fig. 9. According to the bottom inset, evaluation of Eqs. 2,3 yields an estimate for the minimum achievable device length of 1.02 mm. This is one order of magnitude smaller than the value of 10 mm given in [2] for a conventional two-waveguide nonreciprocal coupler comprising comparable materials and geometry.

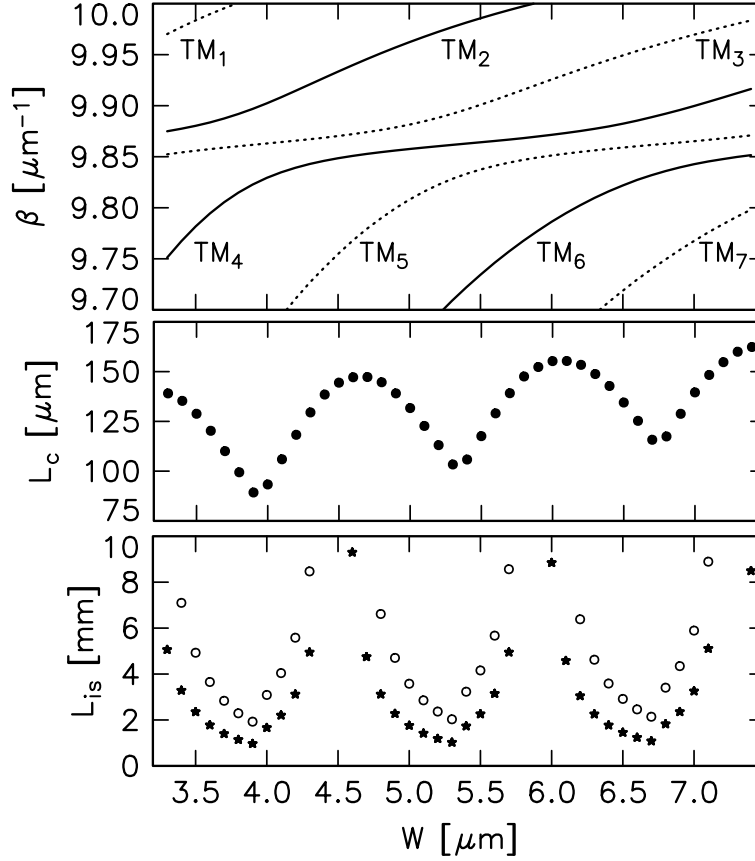


Figure 9: Propagation constants β (top), coupling length L_c (center), and the estimated isolator device length L_{is} (bottom) for TM-polarized light versus the central rib width W of the three rib waveguide coupler. Only part of the region allowed for propagation constants is displayed. Other parameters are as given for Fig. 7, with an off-diagonal permittivity element $\xi = \pm 0.005$. Circles in the bottom chart correspond to a device with isotropic outer guides but a double layer magneto-optic central waveguide, while the stars indicate the total length for a device with both central and outer waveguides made of magneto-optic material as sketched in Fig. 8, with a thickness of the bottom magneto-optic layers of $0.18 \mu\text{m}$.

CONCLUSIONS

For a nonreciprocal three waveguide rib coupler consisting of magneto-optic garnet materials, the proposed design enables standard isolating performance with a total length of about 1 mm. This is achieved by exploiting the specific shape of the relevant mode fields. As in the planar case, strict but manageable tolerance requirements can be expected. Within the complete simulation of the 3-D devices, the numerically involving part of accurately calculating the guided supermodes is by now finished, while the implementation of the propagating mode analysis procedures for the rib waveguide structures is under way.

ACKNOWLEDGMENT

We gratefully acknowledge financial support by Deutsche Forschungsgemeinschaft, Sonderforschungsbereich 225.

REFERENCES

- [1] T. Mizumoto, K. Oochi, T. Harada, and Y. Naito, *Journal of Lightwave Technology*, **4**, (3), pp. 347–352, 1986.
- [2] A. Erdmann, P. Hertel, and H. Dötsch, *Optical and Quantum Electronics*, **26**, pp. 949–955, 1994.
- [3] M. Lohmeyer, M. Shamonin, and P. Hertel, *Optical Engineering*, **36**, (3), pp. 889–895, 1997.
- [4] S. Yamamoto and T. Makimoto, *Journal of Applied Physics*, **45**, pp. 882, 1974.
- [5] M. Lohmeyer, *Optical and Quantum Electronics*, **29**, pp. 907–922, 1997.